Biophysical Chemistry 17 (1983) 57–65
Elsevier Biomedical Press

SIMULATION OF CONVOLUTED AND EXACT EMISSION ANISOTROPY DECAY PROFILES

J. PAPENHUIJZEN * and A.J.W.G. VISSER **

Department of Biochemistry, Agricultural University, 6703 BC Wageningen, The Netherlands

Received 25th January 1982
Revised manuscript received 20th September 1982
Accepted 23rd September 1982

Key words: Anisotropy decay; Fluorescence decay; Rotational correlation time; Deconvolution

We have simulated the convolution of the emission anisotropy decay function with both a δ-pulse excitation function (exact solution) and a pulse function of either Gaussian or other functional form. It can be readily shown that convolution with a pulse of finite width leads to lower r_0 values (anisotropy at time zero). Especially in the case of short-lived fluorescence, it can be demonstrated that the convoluted anisotropy lags behind the exact anisotropy leading to longer apparent rotational correlation times. Contour plots of r corrections as a function of both fluorescence lifetime and rotational correlation time were constructed for two different pulse profiles. Inspection of these contour diagrams can lead to an estimate of the relative error involved, when anisotropy data are not deconvoluted.

1. Introduction

Rotational diffusion coefficients of macromolecules in solution can be determined from the time dependence of the emission anisotropy of internal or external fluorophores [1–3]. Ideally, this is achieved by exciting a fluorescent reporter group in the macromolecule with a δ-shaped (Dirac) or infinitely short pulse of plane polarized light. The time evolution of fluorescence intensities parallel ($I_{\parallel}(t)$) and perpendicular ($I_{\perp}(t)$) to the electrical vector of the excitation pulse yields the ideal anisotropy decay function $r(t)$:

$$r(t) = \frac{I_{\parallel}(t) - I_{\perp}(t)}{I_{\parallel}(t) + 2I_{\perp}(t)} = \frac{d(t)}{s(t)} \tag{1}$$

Fluorescence emission can be considered as a first-order rate process. The total fluorescence decay ($s(t)$) is therefore represented by a single or multiple exponential function, depending on local environmental inhomogeneities or on the presence of different fluorescent species (see ref. 1):

$$s(t) = \sum_{i=1}^{n} a_i \exp(-t/\tau_i) \tag{2}$$

where n is the number of components, a_i the relative intensity contribution and τ_i the fluorescence lifetime of component i.

In a homogeneous environment with only one fluorescent species present, the anisotropy decay function can be written as a sum of exponentials as shown by Tao [4]. The exact number of exponentials in this case depends on the asymmetry of the macromolecule and amounts to maximally five for an asymmetric rotor [5]. Small and Isenberg [6] demonstrated that in practice three or less exponentials are sufficient:

$$r(t) = \sum_{j=1}^{3} b_j \exp(-t/\phi_j) \tag{3}$$

* Present address: Department of Physical and Colloid Chemistry, Agricultural University, Wageningen, The Netherlands.
** To whom correspondence should be addressed.

0301-4622/83/0000–0000/$03.00

where b_j represents the relative contribution of the anisotropy decay with rotational correlation time ϕ_j to the overall decay $r(t)$. From eqs. 1–3 it follows that $d(t)$ can also be written as a sum of exponentials, with time constants $(1/\tau_i + 1/\phi_j)^{-1}$ that can be considered as combinations of pairs of τ_i and ϕ_j.

The preceding equations only hold when the excitation pulse is infinitely short. In practice, the excitation source generates pulses of finite width. Using the technique of time-correlated single-photon counting and a mode-locked Ar ion laser [7], pulse widths of the order of 0.3–0.5 ns are obtained and this should be taken into account in the analysis of subnanosecond motion. It implies that the convolution products of $s(t)$ and $d(t)$, respectively, with the apparatus response function $g(t)$ should be considered [1]:

$$S(t) = \int_{t_{min}}^{t} g(t')s(t-t')\mathrm{d}t' \tag{4a}$$

$$D(t) = \int_{t_{min}}^{t} g(t')d(t-t')\mathrm{d}t' \tag{4b}$$

The experimental time-dependent anisotropy now follows with eqs. 4a and 4b as:

$$R(t) = \frac{D(t)}{S(t)} \tag{5}$$

which is a quotient of two convolution products. A priori it is not obvious how the finite pulse width of $g(t)$ affects the experimental anisotropy $R(t)$ as compared to the true one, $r(t)$. The instrumental response function is definitely not cancelled in the quotient of eq. 5.

A numerical deconvolution method to retrieve $r(t)$ from $R(t)$ was described by Wahl [8]. Test functions $R(t)$ were obtained from exact expressions for $r(t)$ and $s(t)$, by convolving them with two different experimental functions $g(t)$.

In this study the differences between $r(t)$ and $R(t)$ are more closely investigated. The functions $D(t)$ and $S(t)$ are computed analytically from exact expressions for the response function. Using this approach it is possible to examine visually the conditions under which significant differences between the theoretical $r(t)$ and the experimental $R(t)$ occur. In addition, for the case of mono-exponential fluorescence and anisotropy decays the relative deviation between apparent and true anisotropy decay is presented in the form of contour plots. One can then formally decide whether or not experimental data have to be deconvoluted. In order to achieve this simulation two computer programs were developed.

2. Methods

Exact expressions for $S(t)$ and $D(t)$ are derived using two different pulse profiles of identical peak height and pulse width:

(1) A Gaussian pulse, which is representative for the shape of a mode-locked laser pulse:

$$g(t) = 0.5\exp(-At^2) \tag{6}$$

This function reaches its peak value 0.5 for $t = 0$. The parameter A (in s^{-2}) is inversely related to the pulse width w at half height through

$$A = \frac{\ln 16}{w^2} \tag{7}$$

(2) A modification of the pulse function as used by McKinnon et al. [9] and by Duddeli [10], exhibiting a 'tail' and representative for the pulse profile of spark gap discharge lamps:

$$g(t) = \frac{e^2A^2}{8}\left(t + \frac{2}{A}\right)^2 \exp\left[-A\left(t + \frac{2}{A}\right)\right] \tag{8}$$

This expression also has its maximum 0.5 for $t = 0$ and again the parameter A (now in s^{-1}) is inversely related to w. However, no analytical expression can be derived and therefore A is evaluated numerically from a given value of w.

As indicated in section 1, the convolution product of $d(t)$ or $s(t)$ with $g(t)$ can generally be written as:

$$\begin{aligned} F(t) &= \int_{t_{min}}^{t} g(t')\sum_i \alpha_i \exp(-\beta_i(t-t'))\mathrm{d}t' \\ &= \sum_i \int_{t_{min}}^{t} g(t')\alpha_i \exp(-\beta_i(t-t'))\mathrm{d}t' \end{aligned} \tag{9}$$

with $F(t)$ representing either $D(t)$ or $S(t)$ and α_i, β_i parameters of $d(t)$ or $s(t)$.

Thus, it is sufficient to derive a general expression for the convolution product of $g(t)$ with a single exponential. Substitution of various sets of

parameter values (α_i, β_i) in eq. 9 then yields exact expressions for $D(t)$ and $S(t)$.

The convolution product of a Gaussian excitation pulse with a single-exponential function is obtained by substitution of eq. 6 for $g(t')$ with $t_{min} = -\infty$:

$$\tfrac{1}{2}\int_{-\infty}^{t} \exp\{-A(t')^2\}\alpha \exp\{-\beta(t-t')\}dt'$$

$$= \frac{\alpha}{2}\sqrt{\frac{\pi}{A}} \exp\left(\frac{\beta^2}{4A} - \beta t\right)\int_{-\infty}^{k} \frac{1}{\sqrt{2\pi}} \exp(-r^2/2)dr \qquad (10)$$

with

$$k = t\sqrt{2A} - \frac{\beta}{2\sqrt{A}}$$

The integral on the right-hand side of eq. 10 is a standard Gaussian integral, which has been tabulated [11] or can be computed using standard subroutines (e.g., see ref. 12).

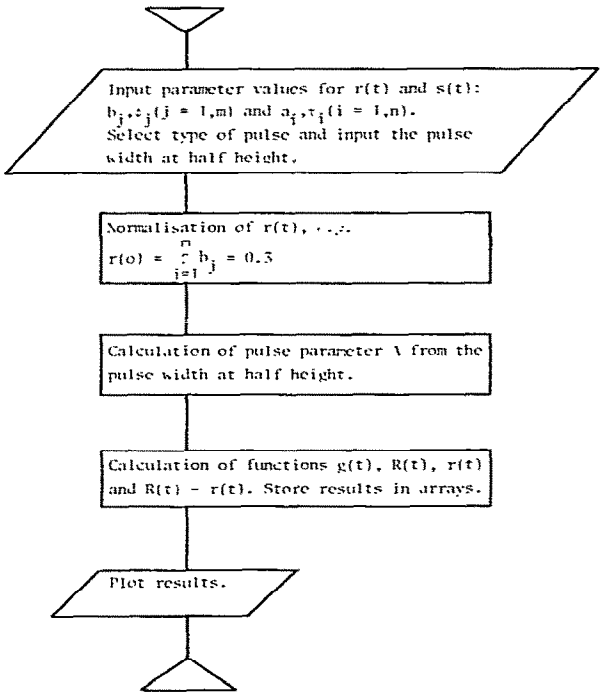

Fig. 1. Flow chart of computer program for the generation of plots representing ideal and convoluted anisotropy decay. Examples are shown in figs. 3–7.

Substitution of the tail excitation pulse (eq. 8) for $t_{min} = -2/A$ into eq. 9 yields the following expression for a single exponential:

$$\frac{e^2A^2}{8}\int_{-\frac{2}{A}}^{t}\left(t'+\frac{2}{A}\right)^2 \exp\left\{-A\left(t'+\frac{2}{A}\right)\right\}$$
$$\times \alpha \exp\{-\beta(t-t')\}dt'$$
$$= \frac{e^2A^2}{8}\alpha\left[\frac{-\exp\{-(At+2)\}}{A-\beta}\left(t+\frac{2}{A}\right)^2\right.$$
$$-\frac{2\exp\{-(At+2)\}}{(A-\beta)^2}\left(t+\frac{2}{A}\right)$$
$$\left.-\frac{2\exp\{-(At+2)\}}{(A-\beta)^3}+\frac{2\exp\left\{-\beta\left(t+\frac{2}{A}\right)\right\}}{(A-\beta)^3}\right] \qquad (11)$$

In the limiting case $A = \beta$ a simpler expression is found:

$$\frac{e^2A^2}{8}\int_{-\frac{2}{A}}^{t}\left(t'+\frac{2}{A}\right)^2 \alpha \exp\{-(At+2)\}dt'$$

$$= \frac{e^2A^2}{24}\alpha \exp\{-(At+2)\}\left(t+\frac{2}{A}\right)^3 \qquad (12)$$

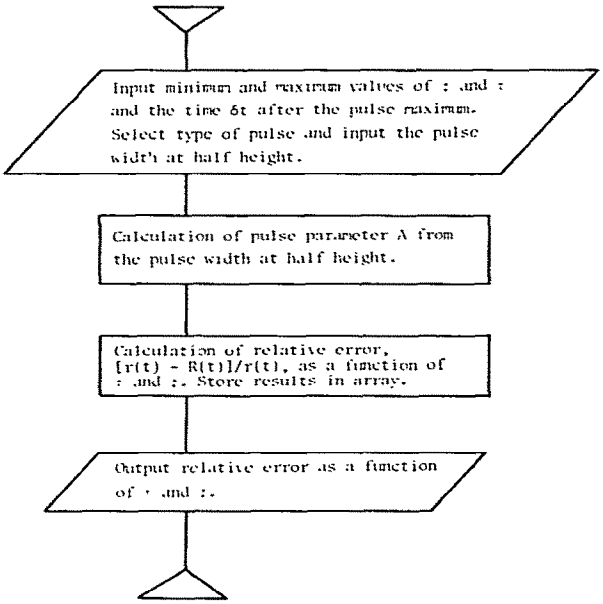

Fig. 2. Flow chart of computer program to calculate points of contour plots, giving a more general impression of the relative error in convoluted anisotropy decay as compared to the ideal case. Examples are shown in fig. 8.

A computer program was written in order to plot the functions $g(t)$, $r(t)$ and $R(t)$, respectively, and also the difference $R(t)-r(t)$. Standard subroutines [12] were used to perform some calculations (A in eq. 8 and the integral in eq. 10) and the plots were generated using a package of graphic subroutines [13]. A flow chart of this program is presented in fig. 1.

For the generation of contour plots the computer program described in fig. 1 was modified in such a way that relative deviations $\{r(t)-R(t)\}/r(t)$ are calculated as a function of ϕ/w and τ/w, respectively. The time δt after the excitation pulse maximum is preset and can be given any value between zero and infinity. From the calculated data contour plots can be constructed with the desired accuracy, as the spacing between successive values of τ/w and ϕ/w can be freely chosen. A flow chart of this program is shown in fig. 2.

3. Results

Only rotational correlation times determine the ideal anisotropy $r(t)$, when the initial anisotropy ($=r_0$) is known. However, the shape of a convoluted function $R(t)$ not only varies with these rotational correlation times, but also with pulse shape and fluorescence lifetimes. This is illustrated

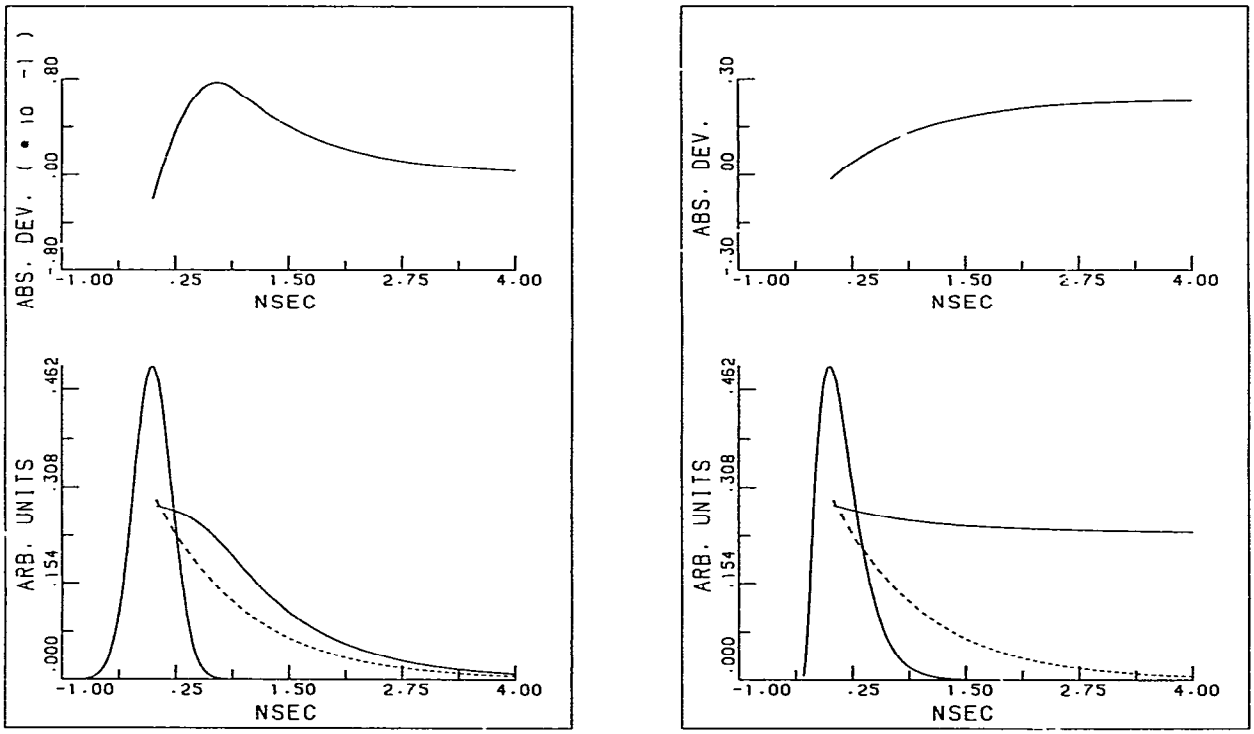

Fig. 3. Lower panel: pulse response function (———), ideal (— — —) and nonideal (———) anisotropy decay. Top panel: absolute difference $R(t)-r(t)$. Left: results obtained with Gaussian excitation pulse. Right: results obtained with excitation pulse containing a tail (see text). Parameter values: rotational correlation time $\phi = 1.0$ ns and fluorescence lifetime $\tau = 0.1$ ns, pulse width at half height $w = 0.5$ ns.

by $R(t)$ plots generated from single-exponential functions $r(t)$ and $s(t)$. The initial anisotropy r_0 is normalized to 0.3, lower than the maximum value of 0.4. Each figure compares the function $R(t)$ calculated with the two mentioned pulse response functions, having an arbitrary peak value of 0.5 at zero time. The pulse width of 0.5 ns is representative for the pulses generated and detected by a mode-locked Ar ion laser/single-photon counting system [7]. Figs. 3–5 present a selection of the results. In figs. 3 and 4 the fluorescence lifetimes τ are varied, whereas figs. 4 and 5 demonstrate how different rotational correlation times ϕ influence the results. If the lifetime is much shorter than the pulse width (fig. 3), the discrepancy between exact and convoluted anisotropy is larger. A Gaussian pulse profile induces a delay in the anisotropy decay, whereas the results obtained with a tail pump function are even more out of proportion. A longer fluorescence lifetime (fig. 4) does improve the results. From the absolute differences between $R(t)$ and $r(t)$ it can be concluded that the initial anisotropy R_0 is lower than the true one r_0. For the particular set of parameters in fig. 4 the decrease amounts to about 10% of r_0. The difference between calculated and ideal anisotropies becomes vanishingly small for longer correlation times (fig. 5); note the expanded scale for the absolute differences.

It should be emphasized that the simulated data are free of noise. Especially the situation depicted in fig. 5 leads in practice to a decay curve in which noise will increse along the decay, since the fluorescence lifetime is relatively short.

Finally, we want to present simulated data related to experiments obtained with fluorescent

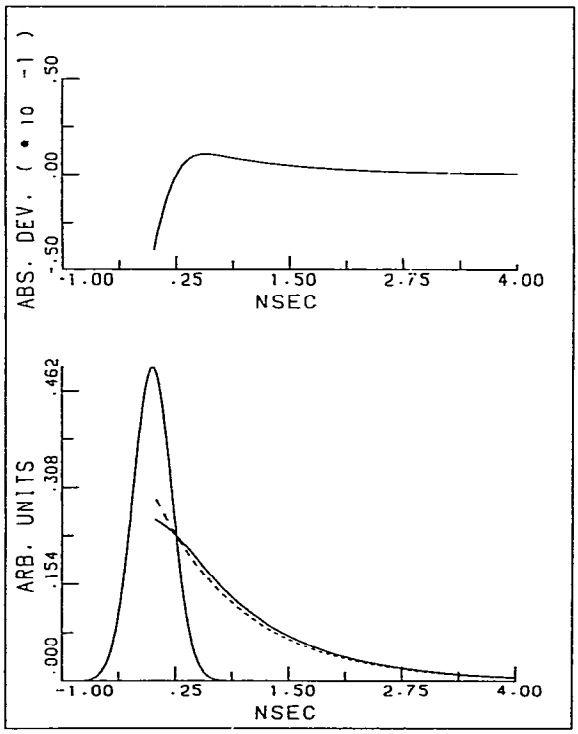

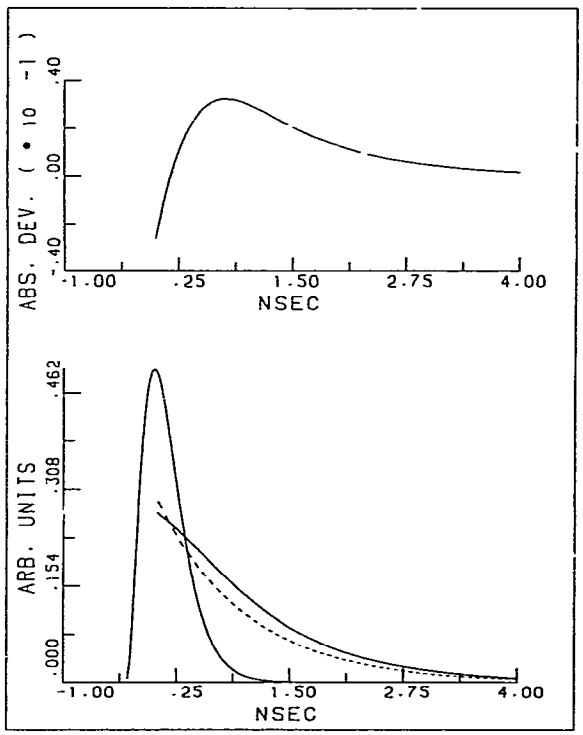

Fig. 4. As fig. 3 except that $\phi = 1.0$ ns and $\tau = 1.0$ ns.

flavins and flavoproteins [14]. Free flavin adenine dinucleotide (FAD) is characterized by a short rotational correlation time (0.46 ns at 10°C) of duration similar to that of the excitation pulse. In this case (fig. 6) deconvolution is required to extract the true value of the correlation time. In the particular case of lipoamide dehydrogenase a rapid subnanosecond motion of bound FAD is superimposed on the protein rotation. The experiments carried out at 4 and 40°C were simulated with Gaussian pulse profiles (fig. 7). From the absolute differences in the experiment at 40°C it can be observed that it is difficult to determine the low amplitude of the rapid motion within the limited experimental time scale.

One should be careful in interpreting observed subnanosecond relaxation processes, as a 0.5 ns pulse width (w) is usually found for mode-locked laser pulses in combination with single-photon counting detection. In order to draw more general conclusions from our simulation method we have generated contour plots for both pulse forms. In these plots we portrayed the values of τ/w vs. those of ϕ/w for certain values of the relative error in the anisotropy, $\{r(t) - R(T)\}/r(t)$. Calculations were performed at two distinct times (δt) after the pulse maximum. Firstly, contours were made at $\delta t = 0$. This set of curves yields the relative error in the initial anisotropy. The second set of curves was obtained at a time $\delta t = w$. These results are collected in the four graphs of fig. 8. The four sets of curves in fig. 8 give a general impression of the errors involved, when experimental anisotropy decay curves are approximated by corresponding ideal functions.

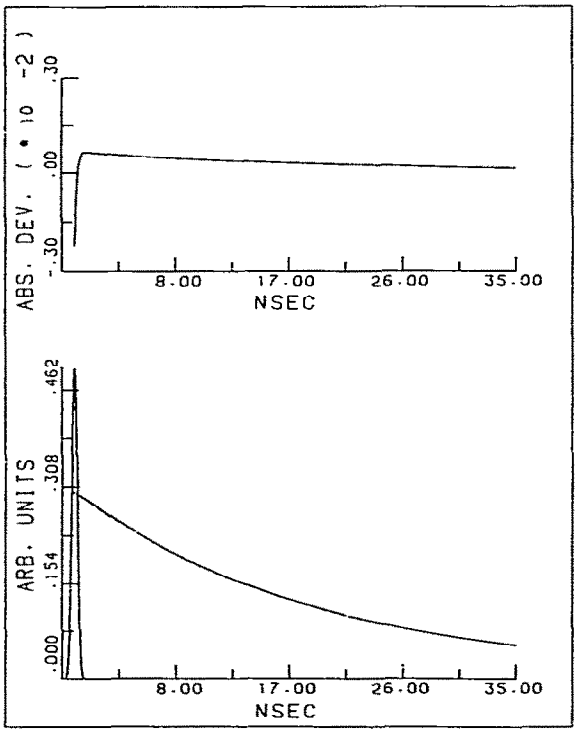

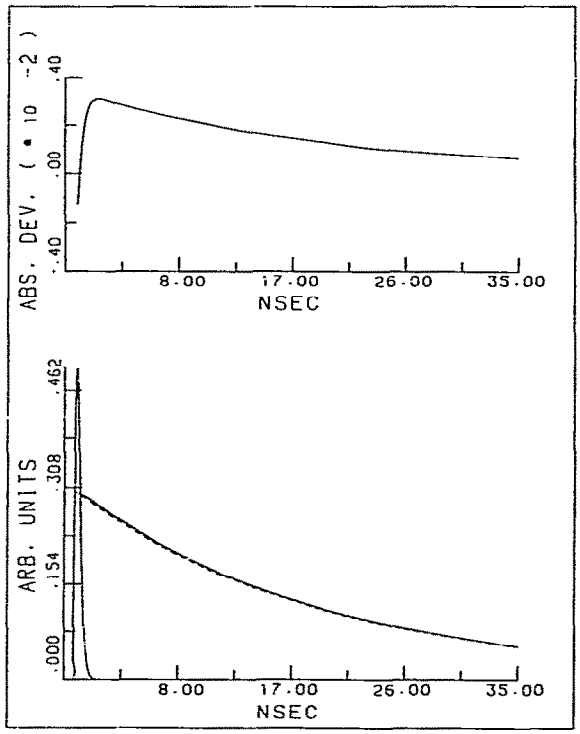

Fig. 5. As fig. 3 except that $\phi = 20.0$ ns and $\tau = 1.0$ ns.

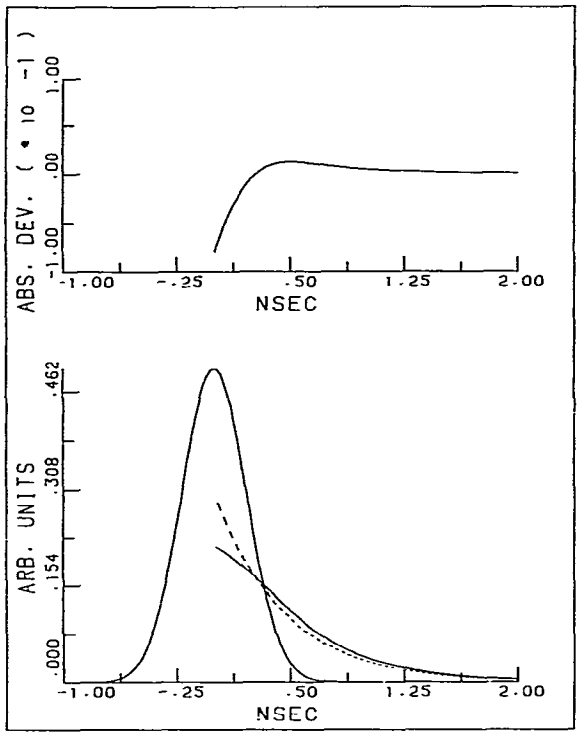

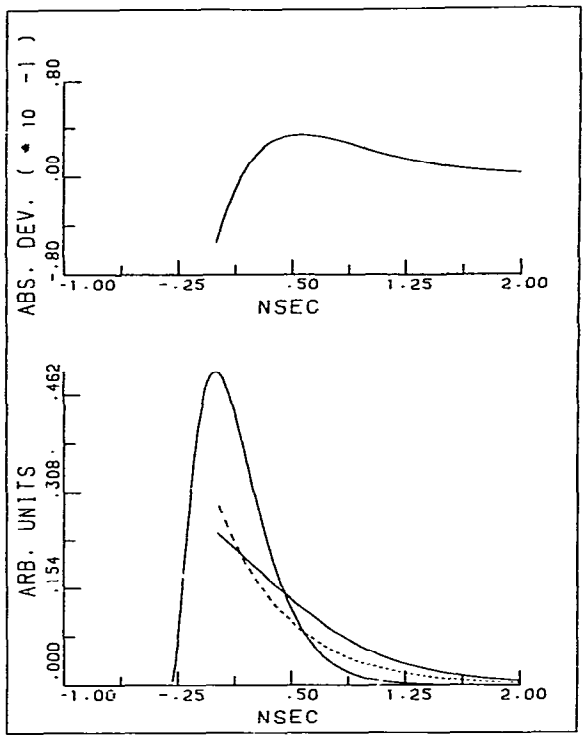

Fig. 6. As fig. 3 except that $\phi = 0.46$ ns and $\tau = 3.0$ ns (FAD in H_2O at 10°C).

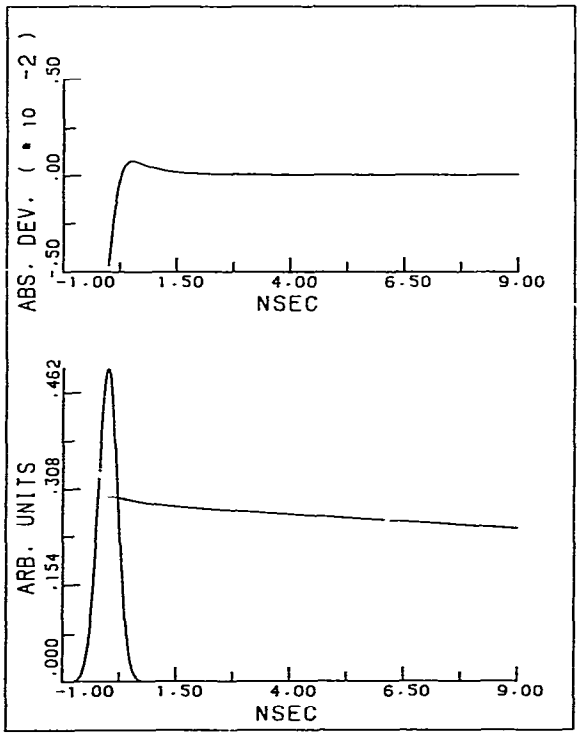

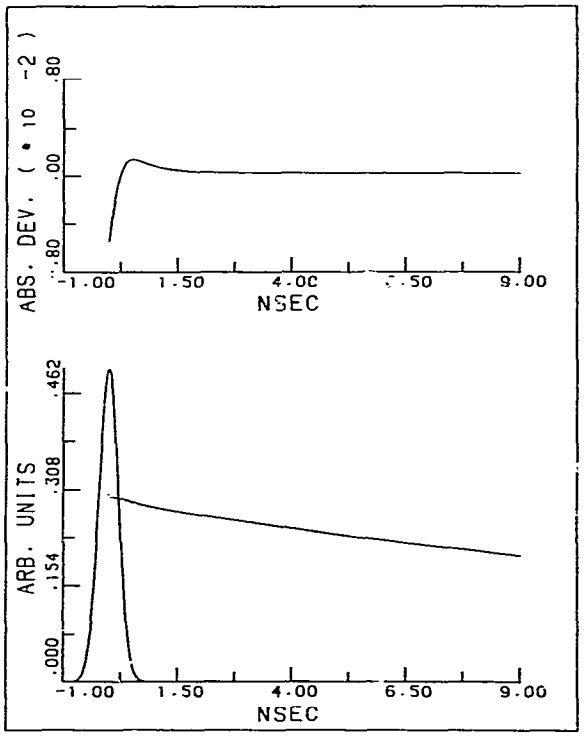

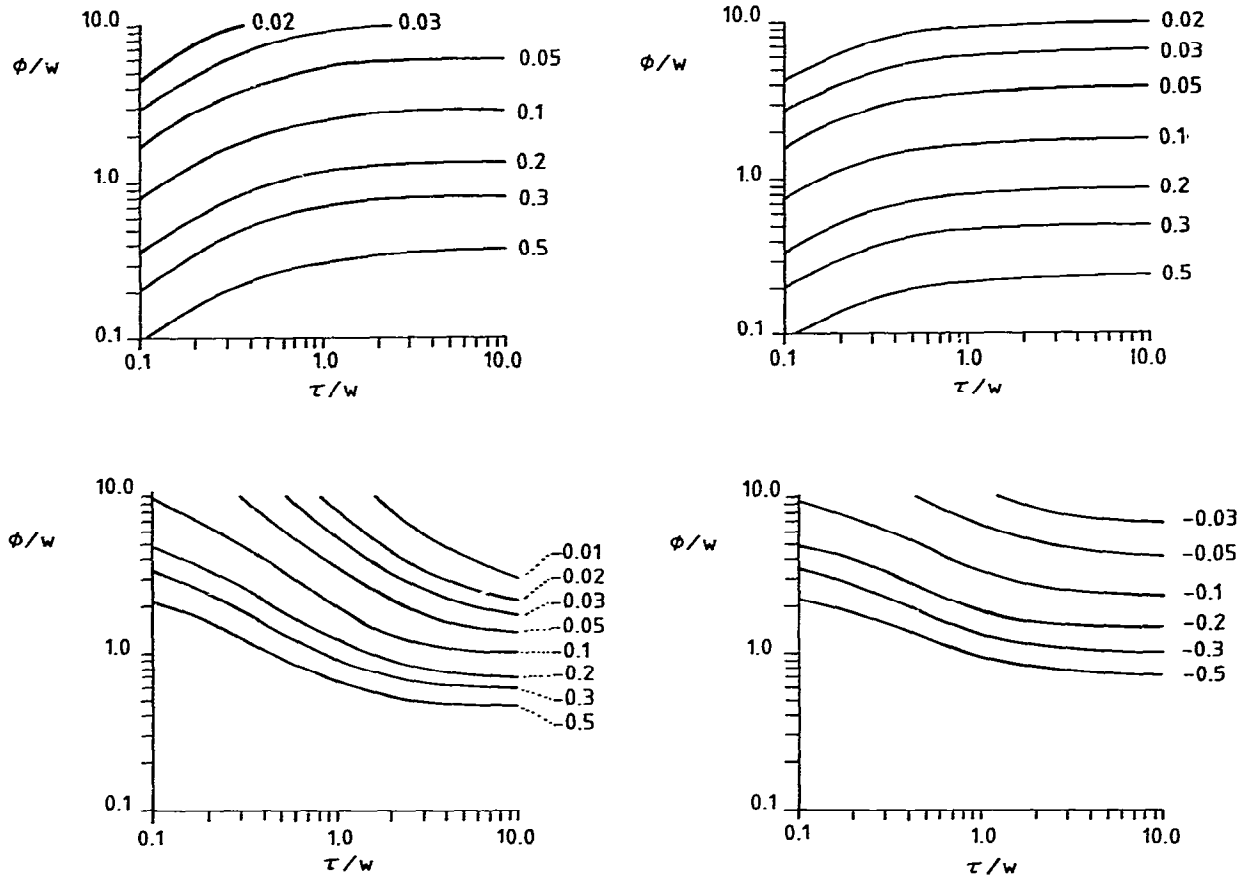

Fig. 8. Contour diagrams describing the relative deviation of the apparent anisotropy R from the true one r. Contour plots are shown for ϕ/w (ordinate) against τ/w (abscissa) at constant relative error, $(r(t)-R(t))/r(t)$, indicated at each curve. Four sets of curves are shown. The top two curves represent r_0 corrections at the excitation maximum, $\delta t = 0$. The lower two curves are for r corrections at a time $\delta t = w$ after the excitation maximum. Left: results with Gaussian excitation pulse. Right: results with excitation pulse containing tail.

4. Conclusion

From an appraisal of the presented figures one can arrive at the following conclusions. The initial anisotropy R_0 is lower than the ideal one r_0, when the pulse response function $g(t)$ is of finite width, regardless of its shape. The pulse evidently influences the measured anisotropy decay. A shorter fluorescence lifetime results in larger differences between ideal and nonideal anisotropy decay; longer correlation times cannot be determined if the fluorescence lifetime is too short. When the

Fig. 7. Simulations of anisotropy decay of lipoamide dehydrogenase [14]. Left: at 4°C with $\phi_1 = 0.5$ ns, $\phi_2 = 57$ ns and $b_1/b_2 = 0.054$; $\tau_1 = 0.6$ ns, $\tau_2 = 4.1$ ns and $a_1/a_2 = 0.563$. Right: at 40°C with $\phi_1 = 0.5$ ns, $\phi_2 = 26$ ns and $b_1/b_2 = 0.054$; $\tau_1 = 0.5$ ns, $\tau_2 = 2.0$ ns and $a_1/a_2 = 1.041$. Only convolutions with Gaussian excitation pulses ($w = 0.5$ ns) are presented.

correlation time is shorter than the pulse width the difference between ideal and nonideal anisotropy increases and $r(t)$ has to be calculated from $R(t)$. For longer correlation times $R(t)$ is a reasonable approximation of $r(t)$. Fig. 8 gives a more general impression of the relative errors involved in experimental anisotropy decay curves as compared to the ideal case.

In cases where the fluorescence lifetime is shorter than the pulse width, Wahl [8] found that the nonideal anisotropy passes through a minimum. In this work this could not be confirmed (cf. fig. 3). A possible explanation is the very pronounced tail of the experimental pulse response function as employed by Wahl [8].

Acknowledgements

We thank Miss Lyda Verstege for preparation of the typescript. This work was supported in part by the Netherlands Foundation for Chemical Research (SON) with financial aid from the Netherlands Organization for the Advancement of Pure Research (ZWO).

References

1 R. Rigler and M. Ehrenberg, Q. Rev. Biophys. 6 (1973) 134.
2 J. Yguerabide, Methods Enzymol. 26, C (1972) 98.
3 P. Wahl, in: Concepts in biochemical fluorescence, vol. 1, eds. R.F. Chen and H. Edelhoch (Marcel Dekker, New York, 1975) p. 1.
4 T. Tao, Biopolymers 8 (1969) 609.
5 G.G. Belford, R.L. Belford and G. Weber, Proc. Natl. Acad. Sci. U.S.A. 69 (1972) 1392.
6 E.W. Small and I. Isenberg, Biopolymers 18 (1977) 1907.
7 A.J.W.G. Visser and A. van Hoek, J. Biochem. Biophys. Methods 1 (1979) 195.
8 P. Wahl, Biophys. Chem. 10 (1979) 91.
9 A.E. McKinnon, A.G. Szabo and D.R. Miller, J. Phys. Chem. 81 (1977) 1564.
10 D.A. Duddell, Photochem. Photobiol. 31 (1980) 121.
11 M. Abramowitz and I.A. Stegun, Handbook of mathematical functions (Dover Publications, New York, 1972).
12 'International Mathematical and Statistical Library', IMSL, Inc., Houston, TX (1980).
13 'Komplot', Communications No. 7, January 1977, Computer Center, University of Groningen, Groningen, The Netherlands.
14 A.J.W.G. Visser, H.J. Grande and C. Veeger, Biophys. Chem. 12 (1980) 35.